A hybrid real-time command governor supervisory scheme for constrained control systems

Domenico Famularo, *Member, IEEE*, Giuseppe Franzè, *Member, IEEE*, Angelo Furfaro, *Member, IEEE* and Massimiliano Mattei, *Senior Member, IEEE*

***Abstract*—In this paper we develop a hybrid supervisory control architecture in a real-time environment for constrained control systems. The strategy is based on Command Governor (CG) ideas that are here specialized in order to jointly take into account time-varying set-points and constraints. The significance of the method mainly lies in its capability to avoid constraints violation and loss of stability regardless of any configuration change occurrence in the plant/constraint structure by replacing the current CG with a new on-line computed unit. A real-time scheme is an extremely appealing choice because of its numerous engineering applications: automobile industry, defense and aerospace, chemical and nuclear plant applications, multimedia/telecommunications and so on. Experimental results on a laboratory four-tank test-bed and simulations on a Cessna 182 aircraft model show the effectiveness of the proposed strategy.**

I. Introduction

The complexity of nowadays computer controlled systems arises from the engineering requirement to properly merge and integrate actuators, sensors and computing units because the related signal processing and feedback control tasks are accomplished within complex and distributed data network structures, see e.g. [21]).

The resulting feedback setup is then quite "large" and is expected to adapt in a timely, rapid and correct fashion to frequently changing environment variables and conditions. It must be noted that modern computer architectures, usually (highly) parallel, often distributed, using many heterogeneous resources need to be designed to properly operate for decades, due in part to the tremendous cost of their development. As a consequence, a computer controlled system needs to incorporate, in accordance with the requirements of the chosen application, a wide variety of often conflicting functional/non-functional objectives and it is then natural to characterize all these setups within a real-time framework [34], [29].

Examples of real-time applications are numerous in literature ranging from manufacturing control, robot operations in hazardous environments or life-threatening situations, cruise control in cars and planes, multimedia/telecommunications, surveillance/monitoring etc. [21], [24], [12]. The main motivations behind a real-time control scheme can be summarized as: complex and often conflicting objectives (such as functionality, timeliness, fault-tolerance), a significant parallelism degree and, in some cases, the integration of multiple existing large scale systems.

Strictly speaking, a real-time control system is an algorithmic structure in which the soundness of a result not only depends on its logical/formal computational correctness but also upon the time instant when the result is made available [15]. Huge number of sensors/actuators, nonlinear phenomena, undesired effects due to switching operating conditions as well as physical constraints due to input/state saturations are of paramount relevance when implementing a real-time control strategy for complex plants. In literature the most popular paradigms proposed for real-time applications are based on adaptive/soft computing algorithms, extremely useful in case of severe plant nonlinearities due to sudden switchings and fault/failures occurrences (see [22] and references therein), and predictive schemes which can efficiently cope with the presence of constraints and nonlinear dynamics [14], [27], [33], [26], [25].

The contributions of Wang and Boyd [33] and Miksch *et al.* [26] are here of interest when referring to MPC strategies: in the first a Quadratic Programming (QP) algorithmic technique to significantly speed up the computation time of on-line MPC schemes is outlined. It is proved that for a large number of plant states and constraints the proposed computational scheme is easily customizable to work within a real-time convex optimization scheme. In the second contribution the reconfiguration capabilities of a real-time MPC scheme in presence of faults in the plant structure are analyzed in details.

The main contribution of this paper is to develop a real-time implementation of a low-computational demanding predictive scheme known in literature as the command governor (CG) (see [3], [5], [17]) for the supervision of nonlinear dynamical systems subject to sudden switchings amongst operating and set-points and time-varying constraint paradigms by preserving its basic properties. It is worth to underline that, despite the availability of high power computational units, the considered time-varying plant structures do not encourage the use of low demanding MPC schemes (see e.g. [6], [33]). The reason is that each MPC initialization due to switching events involves the resolution of Mixed Integer Optimization programs which are a prohibitive task from a computational point of view.

The CG approach is a predictive scheme where stabilization/performance is provided by the primal controller and constraint violation avoidance is separately achieved by the CG strategy. A general framework, capable to take care of the possible plant structure modifications that could take place

Domenico Famularo, Giuseppe Franzè and Angelo Furfaro are with DIMES, Universitá degli Studi della Calabria, Via Pietro Bucci, Cubo 42-C, Rende (CS), 87036, ITALY {famularo,franze,a.furfaro}@dimes.unical.it

Massimiliano Mattei is with DIII - Seconda Università degli Studi di Napoli, Real Casa dell'Annunziata Via Roma, 29, Aversa (CE), 81031, ITALY massimiliano.mattei@unina2.it

during the on-line operations will be considered. The proposed scheme prescribes that any change in the plant structure affects the CG design and, as a consequence, for each plant structure variation a different CG unit should be in principle designed complying with the new conditions. The idea is then that a suitable supervisory unit must be designed to take care of orchestrating the switching amongst the CG candidates during the on-line operations.

A real-time implementation of the previously described scheme is then proposed and summarized. At the generic instant the plant is under the action of a given CG and the supervisory unit acquires information on the plant structure to be fulfilled at the next time instant. A sequence of evaluations and switching rules are taken according to a finite state machine which describe the situations of normal operating conditions, handling of a set-point and/or equilibrium change event and handling of a constraint configuration change event. The supervisor component is managed by a single periodic task which runs at the highest priority level and it is in charge to execute all the necessary CG operations (reference/state measurement, modified CG command computation and primal controller executions). This is achieved by means of a C++ implementation of the CG algorithm (see [13], [31]) on a software platform based on a RTAI/Linux kernel which is a software hard real-time extension for the Linux kernel allowing to intercept the system calls and to emulate them.

II. The Command Governor (CG) design

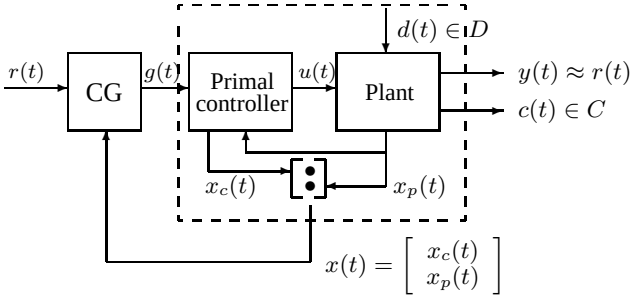

Fig. 1. Command Governor structure

In Fig. 1 the basic reference governor scheme with the model plant, the primal controller and the CG device is depicted. We will suppose that the closed-loop plant regulated by the primal controller is linearized around a given equilibrium and discretized as

$$\begin{cases} x(t+1) &= \Phi x(t) + Gg(t) + G_d d(t) \\ y(t) &= H_y x(t) \\ c(t) &= H_c x(t) + Lg(t) + L_d d(t) \end{cases} \quad (1)$$

where $x(t) \in \mathbb{R}^n$ ($t \in \mathbb{Z}_+$) is the overall state including the plant and primal controller states; $g(t) \in \mathbb{R}^m$ is the CG action, i.e. a suitably modified version of the reference signal $r(t) \in \mathbb{R}^m$; $d(t) \in \mathcal{D} \subset \mathbb{R}^{n_d}$, $\forall t \in Z_+$ is an exogenous disturbance, with $\mathcal{D}$ a specified convex and compact set such that $0_{n_d} \in \mathcal{D}$; $y(t) \in \mathbb{R}^m$ is the plant output which is required to track $r(t)$; $c(t) \in \mathbb{R}^{n_c}$ the constrained output vector

$$c(t) \in \mathcal{C}, \ \ \forall t \in \mathbb{Z}_+ \quad (2)$$

with $\mathcal{C}$ a specified convex and compact set. It is also assumed that:

Assumption A1 -

$$\begin{cases} 1) & \Phi \text{ is a Schur matrix} \\ 2) & \text{The model plant (1) is offset-free, i.e.} \\ & H_y(I_n - \Phi)^{-1}G = I_m \end{cases}$$

Observe that the typical structure of a CG-equipped control system consists of two nested loops. The internal loop is designed via a generic linear control method, without taking into account the prescribed constraints, and allows the designer to specify relevant system properties for small-signal regimes, e.g. stability, disturbance rejection. The outer loop consists of the CG unit which, whenever necessary, is in charge to modify the reference to be applied to the closed-loop system so as to avoid constraint violation. The basic idea is that of maintaining the closed-loop system within its nominal linear regime, where the stability and all other closed-loop properties are preserved.

The CG design problem is that of generating, at each time instant t, the set-point $g(t)$ as a function of the current state $x(t)$ and reference $r(t)$

$$g(t) := \overline{g}(x(t), r(t)) \quad (3)$$

in such a way that, regardless of disturbances, constraints (2) are always fulfilled along the system trajectories generated by the application of the modified set-points $g(t)$ and possibly $y(t) \approx r(t)$. Moreover, it is required that: $g(t) \to \hat{r}$ whenever $r(t) \to \hat{r}$, where $\hat{r}$ is either r or its best feasible approximation; the CG has a finite settling time, viz. $g(t) = \hat{r}$ for a possibly large but finite t whenever the reference stays constant after a finite time. By linearity, it is possible to separate the effects of the initial conditions and input from those of disturbances, i.e. for each generic system variable $n(t)$: $n(t) = \overline{n}(t) + \tilde{n}(t)$, where $\overline{n}(t)$ is the disturbance-free component and $\tilde{n}(t)$ depends only on disturbances. Therefore, the disturbance-free solutions of (1) to a constant command $g(t) = w$ are:

$$\begin{array}{rcl} \overline{x}_w &:=& (I_n - \Phi)^{-1}Gw \\ \overline{y}_w &:=& H_y(I_n - \Phi)^{-1}Gw \\ \overline{c}_w &:=& H_c(I_n - \Phi)^{-1}Gw + Lw \end{array} \quad (4)$$

Consider next the following set recursions:

$$\mathcal{C}_0 := \mathcal{C} \sim L_d\mathcal{D},$$
$$\mathcal{C}_k := \mathcal{C}_{k-1} \sim H_c\Phi^{k-1}G_d\mathcal{D}, \ \ldots, \mathcal{C}_\infty := \bigcap_{k=0}^{\infty} \mathcal{C}_k,$$

where $\mathcal{A} \sim \mathcal{E}$ is defined as $\{a : \ a + e \in \mathcal{A}, \forall e \in \mathcal{E}\}$, see e.g. [8]. It can be shown that the sets $\mathcal{C}_k$ are nonconservative restrictions of $\mathcal{C}$ such that $\overline{c}(t) \in \mathcal{C}_\infty, \forall t \in \mathbb{Z}_+$, implies that $c(t) \in \mathcal{C}, \forall t \in \mathbb{Z}_+$. Thus, one can consider only disturbance-free evolutions of the system and adopt a "worst-case" approach. For reasons which will appear clear soon, it is convenient to introduce the following sets for a given $\delta > 0$

$$\mathcal{C}^\delta := \mathcal{C}_\infty \sim \mathcal{B}_\delta \quad (5)$$
$$\mathcal{W}^\delta := \left\{w \in \mathcal{R}^m : \ \overline{c}_w \in \mathcal{C}^\delta\right\} \quad (6)$$

where $\mathcal{B}_\delta$ is a ball of radius δ centered at the origin. We shall assume that there exists a possibly vanishing $\delta > 0$

such that $\mathcal{W}^\delta$ is non-empty. In particular, $\mathcal{W}^\delta$ is the set of all commands whose corresponding steady-state solutions satisfy the constraints with a tolerance margin δ. From the foregoing definitions and assumptions, it follows that $\mathcal{W}^\delta$ is closed and convex.

The main idea is to choose at each time step a constant virtual command $g(\cdot) \equiv w$, with $w \in \mathcal{W}^\delta$, such that the corresponding evolution fulfils the constraints over a semi-infinite horizon and its "distance" from the constant reference is minimal. Such a command is applied, a new state is measured and the procedure is repeated. In this respect we define the set $\mathcal{V}(x)$ as

$$\mathcal{V}(x) = \left\{ w \in \mathcal{W}^\delta : \ \overline{c}(k, x, w) \in \mathcal{C}_k, \ \forall k \in \mathcal{Z}_+ \right\} \tag{7}$$

where $\overline{c}(k, x, w) = H_c \left(\Phi^k x + \sum_{i=0}^{k-1} \Phi^{k-i-1} G w \right) + L w$ is the constraint disturbance-free virtual evolution at time k from the initial condition x under the constant command $g(\cdot) \equiv w$. As a consequence $\mathcal{V}(x) \subset \mathcal{W}^\delta$, and, if non-empty, it represents the set of all constant virtual sequences in $\mathcal{W}^\delta$ whose evolutions starting from x satisfies the constraints also during transients. Thus the CG output is chosen according to the solution of the following constrained optimization problem

$$g(t) = \arg \min_{w \in \mathcal{V}(x(t))} \|w - r(t)\|_\Psi \tag{8}$$

where $\Psi = \Psi^T > 0_m$ and $\|w\|_\Psi := w^T \Psi w$.

A detailed discussion about the CG approach and its main properties can be found in [5]. For specific results on CG see in [16], [17], [3],[4], [1].

III. Hybrid Command Governors

In this section the previous basic CG scheme is generalized to time-varying set-points and constraint configurations. To this end, a supervisory based CG framework capable to deal with the plant structure modifications (references and constraint configurations) that could take place during the on-line operations is here described.

Let us consider the plant modelled by a discrete-time nonlinear system

$$x_p(t+1) = f(x_p(t), u(t)) \tag{9}$$

where $x_p(t) \in X \subseteq \mathbb{R}^n$, $u(t) \in U \subseteq \mathbb{R}^m$ denote the plant state and the control input, respectively, X, U being convex and compact sets. It is worth to note that disturbance effects can be also taken into account without compromising all the forthcoming developments.

Under the hypothesis that $f(x, u)$ is continuously differentiable in both its arguments we will assume that the plant (9) could operate in N pre-specified working regions *centered* around N equilibrium points, denoted as $(x_{p_i}^{eq}, u_i^{eq})$, $i = 1, \ldots, N$.

For each operating region we will suppose that the plant dynamics can be approximated around each equilibrium $(x_{p_i}^{eq}, u_i^{eq})$, $i = 1, \ldots, N$, by a corresponding linearized model

$$\delta x_p(t+1) = \quad A_i \, \delta x_p(t) + B_i \, \delta u(t) + F_i(\delta x_p(t), \, \delta u(t))$$

where $A_i = \frac{\partial f}{\partial x_p} \ (x_p, u) \, |_{\left(\begin{smallmatrix} x_p = x_{p_i}^{eq} \\ u = u_i^{eq} \end{smallmatrix}\right)}$ and $B_i = \frac{\partial f}{\partial u}(x_p, u) \, |_{\left(\begin{smallmatrix} x_p = x_{p_i}^{eq} \\ u = u_i^{eq} \end{smallmatrix}\right)}$ are Jacobian matrices with $\delta x_p = x_p - x_{p_i}^{eq}$ and $\delta u = u - u_i^{eq}$. Then $F(\delta x_p, \, \delta u)$ is the Taylor series remainder term and by means of continuity arguments we have that

$$\frac{\|F_i(\delta x_p, \, \delta u)\|_2}{\left\| \left[\delta x_p^T, \, \delta u^T \right]^T \right\|_2} \to 0 \text{ as } \left\| \left[\delta x_p^T, \, \delta u^T \right]^T \right\|_2 \to 0, \tag{10}$$

therefore for any $\gamma^i > 0$ there exist $r^i > 0$ such that

$$\frac{\|F_i(\delta x_p, \, \delta u)\|_2}{\left\| \left[\delta x_p^T, \, \delta u^T \right]^T \right\|_2} < \gamma^i, \ \forall \left\| \left[\delta x_p^T, \, \delta u^T \right]^T \right\|_2 < r^i \tag{11}$$

A. Time-varying set-points

In what follows we will characterize the switching policy of the proposed CG framework. The situation where the references are allowed to belong to a finite levels set (see [2] for details)

$$r \in \mathcal{R} := \{r_1, \ldots, r_q\}, \ r_i \in \mathbb{R}^m, \, i = 1, \ldots, q, \tag{12}$$

is first considered and, for each $i - th$ linearized model a single primal controller/reference governor unit, hereafter termed CG_i, is derived with $\mathcal{W}_i^\delta$, $i \in \mathcal{N} := \{1, 2, \ldots, N\}$, the set of all commands whose corresponding steady-state solutions satisfy the constraint with margin δ.

We make the following tracking assumption for each set point inside $\mathcal{R}$:

A2 -

$$\mathcal{R} \subset \bigcup_{i=1}^{N} \mathcal{W}_i^\delta \tag{13}$$

and $\forall i \in \mathcal{N}$ there exists at least $j \neq i \in \mathcal{N}$ such that

$$Int\{\mathcal{W}_i^\delta \cap \mathcal{W}_j^\delta\} \neq \emptyset \tag{14}$$

where $Int\{\cdot\}$ denotes the set interior operator. □

The key points of the strategy are here summarized:

- a procedure for switching between CG_i and CG_j complying with (14) is defined as follows. By considering the output admissible set for the generic CG_i

$$Z_i^\delta := \left\{ [r^T, \, x^T]^T \in \mathbb{R}^m \times \mathbb{R}^n | c_i(k, x, r) \in \mathcal{C}, \ \forall k \in \mathbb{Z}_+ \right\} \tag{15}$$

an,d by denoting with $\mathcal{X}_i^\delta$, $i \in \mathcal{N}$, the set of all states, which can be steered to feasible equilibrium points without constraint violation as

$$\mathcal{X}_j^\delta := \left\{ x \in \mathbb{R}^n | \begin{bmatrix} w \\ x \end{bmatrix} \in Z_i^\delta \text{ for at least one } w \in \mathbb{R}^m \right\} \tag{16}$$

we have that

$$Int\{\mathcal{W}_i^\delta \cap \mathcal{W}_j^\delta\} \neq \emptyset \Rightarrow Int\{\mathcal{X}_i^\delta \cap \mathcal{X}_j^\delta\} \neq \emptyset, \quad i, j \in \mathcal{N} \tag{17}$$

The validity of (17) directly follows from standard viability arguments, see [5]. Therefore, a convenient transition reference $\hat{r} \in Int\{\mathcal{W}_i^\delta \cap \mathcal{W}_j^\delta\}$, with $\hat{x} \in Int\{\mathcal{X}_i^\delta \cap \mathcal{X}_j^\delta\}$ the equilibrium steady-state corresponding to $\hat{r}$, can be defined such that $[\hat{r}^T, \ \hat{x}^T]^T \in Z_i^\delta \cap Z_j^\delta$.

- The supervisor maintains CG_i as long as the distance between the equilibrium x_i^{eq} and the actual state $x(t)$ is minimal. On the contrary, it switches to the $j-th$ linear model centered in x_j^{eq} chosen according to

$$j := \arg\min_k \|x_k^{eq} - x(t)\| \tag{18}$$

Then, by assuming that the CG_i unit is in use at $t=\bar{t}$, $r(\bar{t}) \in \mathcal{W}_i^\delta$, $r(\bar{t}+1) \in \mathcal{W}_j^\delta$ and the condition $\mathcal{W}_i^\delta \cap \mathcal{W}_j^\delta \neq \emptyset$ holds true, an HCG scheme can be adopted according to the following switching logic:

Switching procedure -

1) Solve and apply

$$g(\bar{t}+k) := \arg \min_{w \in \mathcal{V}_i(x(\bar{t}+k))} \|w - r(\bar{t})\|_\Psi,\ k = 1, \ldots, \bar{k}$$

2) At $t = \bar{t} + \bar{k}$ as soon as $x(t) \in Int\{\mathcal{X}_i^\delta \cap \mathcal{X}_j^\delta\}$ switch to CG_j and solve

$$g(\bar{t}+k) := \arg \min_{w \in \mathcal{V}_j(x(t))} \|w - r(\bar{t}+1)\|_\Psi,\ t \geq \bar{t}+\bar{k}+1$$

Note that the upper bound $\bar{k}$ to the constraint horizon can be computed off-line with respect to all $x \in X$ in a way similar to that used to determine the CG control horizon, see [5]. The integer $\bar{k}$, exploited during the on-line operations and lasting exactly $\bar{k}$ steps before switching to step 2, ensures that implication (17) holds true from $t = \bar{t} + \bar{k}$ onwards.

B. Time-varying constraint

We will now consider L different constraint scenarios, denoted with $\mathcal{C}_j$, $j \in \mathcal{J} := \{1, 2, \ldots, L\}$, and introduce the following sets doubly indexed w.r.t. to the current couple equilibrium/constraints scenario:

$$\mathcal{W}^\delta_{(\bullet,\ j)} := \{w \in \mathbb{R}^m\ :\ \bar{c}_w \in \mathcal{C}_j^\delta\},\ \forall j \in \mathcal{J} \tag{19}$$

where $\mathcal{W}^\delta_{(\bullet,\ j)}$ (the bullet denotes a fixed equilibrium configuration) is the set of all commands w whose constraints steady-state evolutions satisfy the $j-th$ constraint configuration $\mathcal{C}_j$ with a tolerance margin δ (for notational simplicity we will retain fixed the tolerance margin w.r.t. each constraint configuration). From now on we will assume non-emptyness of $\mathcal{W}^\delta_{(\bullet,\ j)}$, $\forall j \in \mathcal{J}$ and $\mathcal{C}_j^\delta$, $\mathcal{W}^\delta_{(\bullet,\ j)}$ will satisfy the following set overlapping property:

Property 1: Let $(j_1, j_2) \in \mathcal{J}$, then

$$\mathcal{C}_{j_1}^\delta \bigcap \mathcal{C}_{j_2}^\delta \neq \emptyset \Leftrightarrow \mathcal{W}^\delta_{(\bullet,\ j_1)} \bigcap \mathcal{W}^\delta_{(\bullet,\ j_2)} \neq \emptyset \tag{20}$$

The next definitions are then instrumental to characterize all the possible switching features of the sets $\mathcal{C}_j^\delta$ and $\mathcal{W}^\delta_{(\bullet,\ j)}$:

Definition 1: The state $x \in \mathbb{R}^n$ is $\mathcal{C}_j^\delta$*-admissible,* $j \in \mathcal{J}$, if there exists $w \in \mathcal{W}^\delta_{(\bullet,\ j)}$ such that $c(k, x, w) \in \mathcal{C}_j^\delta, \forall k \in \mathbb{Z}_+$. The pair (x, w) is said $\mathcal{C}_j^\delta$*-executable.*

Definition 2: Let $x \in \mathbb{R}^n$ be a state $\mathcal{C}_{j^-}^\delta$*-admissible,* $j^- \in \mathcal{J}$, and $\mathcal{C}_{j^+}^\delta$, $j^+ \neq j^-$, a constraint configuration to be fulfilled at future time instants. The state x is *switching-*$\mathcal{C}_{j^-}^\delta$*-admissible* if there exists $w \in \mathcal{W}^\delta_{(\bullet,\ j^-)}$ such that $c(k, x, w) \in \mathcal{C}_{j^+}^\delta, \forall k \in \mathbb{Z}_+$. The pair (x, w) is said *switching-*$\mathcal{C}_{j^-}^\delta$*-executable* and the constraint configuration $\mathcal{C}_{j^+}^\delta$ *switchable.*

Definition 3: Let $x \in \mathbb{R}^n$ be a state $\mathcal{C}_{j^-}^\delta$*-admissible,* $j^- \in \mathcal{J}$, but not *switching-*$\mathcal{C}_{j^-}^\delta$*-admissible.* Let $\mathcal{C}_{j^+}^\delta$, $j^+ \neq j^-$, be a constraint configuration to be fulfilled at future time instants. The state x is *indirectly-switching-admissible* if the constraint set $\mathcal{C}_{j^+}^\delta$ belongs to the following finite sequence of constraint configuration

$$\mathcal{S}_{sw} := \{\mathcal{C}_{j_1}^\delta, \mathcal{C}_{j_2}^\delta, \ldots, \mathcal{C}_{j_{k-1}}^\delta, \mathcal{C}_{j_k}^\delta\} \tag{21}$$

with $j_1 = j^-$, $j_k = j^+$ and $(\mathcal{C}_{j_1}^\delta, \mathcal{C}_{j_2}^\delta) \ldots (\mathcal{C}_{j_{k-1}}^\delta, \mathcal{C}_{j_k}^\delta)$ *switchable* couples.
Moreover

$$\mathcal{V}_{(\bullet,\ j)}(x) := \{w \in \mathcal{W}^\delta_{(\bullet,\ j)}\ :\ c(k, x, w) \in \mathcal{C}_j^\delta,\ \forall k \in \mathbb{Z}_+\},$$
$$\forall i \in \mathcal{I}$$

represent the sets of all constant virtual sequences in $\mathcal{W}^\delta_{(\bullet,\ j)}$ whose c-evolutions, starting from a $\mathcal{C}_j^\delta$*-admissible* state x, satisfy the prescribed constraint configuration $\mathcal{C}_j^\delta$ also during transients. As a consequence, for a fixed $j \in \mathcal{J}$, $\mathcal{V}_{(\bullet,\ j)}(x) \subset \mathcal{W}^\delta_{(\bullet,\ j)}$. Then, whenever the supervisory unit selects the CG candidate with respect to the j-th constraints configuration ($CG_{(\bullet,\ j)}$), a command $g(t)$ is computed as a solution of the following constrained optimization problem

$$g(t) = \arg \min_{w \in \mathcal{V}_{(\bullet,\ j)}(x(t))} \|w - r(t)\|_\Psi \tag{22}$$

An admissible HCG strategy can then be developed if at each switching instant $\bar{t}$, chosen by the supervisory unit, the current state $x(\bar{t})$ is *switching-admissible* or *indirectly-switching-admissible*. The following sets

$$\begin{aligned}\mathcal{X}^\delta_{(\bullet,\ j)} := \{&x \in \mathbb{R}^n\ :\ c(k, x, w) \in \mathcal{C}_j^\delta,\\ &\text{for at least one } w \in \mathcal{W}^\delta_{(\bullet,\ j)},\ \forall k \in \mathbb{Z}_+\},\ \forall j \in \mathcal{J}\end{aligned} \tag{23}$$

are finally introduced to characterize all the states $\mathcal{C}_j^\delta$*-admissible* (each state $x \in \mathcal{X}^\delta_{(\bullet,\ j)}$ can be steered to an equilibrium point without constraint violation). Key aspects are to verify that the time-varying constraint scenario CG strategy enjoys viability and asymptotic stability properties.

Proposition 1: Consider the plant (1) along with a family of constant command sequences $w \in \mathcal{W}^\delta_{(\bullet,\ j)}$, $j \in \mathcal{J}$, and let $\bar{x}_{\bar{w}}$ be an equilibrium point reached under a constant virtual command $\bar{w} \in \mathcal{W}^\delta_{(\bullet,\ j)}$ from an arbitrary $\mathcal{C}_j^\delta$*-admissible* initial state. Let the assumptions **A1** be fulfilled, the sets $\mathcal{C}_j^\delta$, $\forall j \in \mathcal{J}$ compact and convex, and the sets $\mathcal{W}^\delta_{(\bullet,\ j)}$, $\forall j \in \mathcal{J}$, non-empty, closed and convex. Then, there exists a concatenation of finite virtual constant commands $\bar{w} \in \mathcal{W}^\delta_{(\bullet,\ j)}$, with $j \in \mathcal{J}$, and of constraint configurations $\mathcal{C}_j$ capable of asymptotically driving the plant from $x_{\bar{w}}$ to x_w, where $w \in \mathcal{W}^\delta_{(\bullet,\ j)}$.
Proof - See Appendix A.
It remains to prove that the system (1) under the action of the proposed HCG enjoys the asymptotic stability property.

Proposition 2: Let the assumptions **A1** be fulfilled and the sets $\mathcal{V}_{(\bullet,\ j)}(x(\bar{t}))$, $\forall j \in \mathcal{J}$ be non-empty for any switching time instant $\bar{t}$. It is assumed that there exists a instant time t^* under which the switching of constraint configurations terminates and the reference signal is such that, $r(t) \equiv r$, for all $t \geq \hat{t}$, with $\hat{t} \geq t^*$ and r being a constant value. Then:

$$\lim_{t \to \infty} [g(t+1) - g(t)] = 0_m \tag{24}$$

$$\lim_{t\to\infty}[x(t)-x_{g(t)}]=0_n \tag{25}$$

where $x_{g(t)}=(I-\Phi)^{-1}Gg(t)$. There exits a finite time $t_f>\hat{t}$ such that

$$g(t)=\bar{g}:=\arg\min_{w\in\mathcal{W}^{\delta}_{(\bullet,\ j)}}\|w-r(t)\|_{\Psi},\ \forall t\geq t_f \tag{26}$$

where j being identified as the last constraint configuration activated by the supervisor from t_f onwards.

Proof - The proof follows *mutatis mutandis* the same lines used for the basic CG scheme. For details see [5]. □

Remark 1 - Note that even if the initial and final set-points belong to $\mathcal{W}^{\delta}_{(i,\ j)}$, or the final set-point is fixed in time, the $i-th$ linearized model approximates the nonlinear dynamics (9) only in a neighbouring region of the actual $i-th$ equilibrium point, see e.g. [18]. While the state evolution departs in fact significantly from x_i^{eq}, an obvious performance degradation will take place and a possible way to cope with this drawback is to consider the opportunity to commute the controller structure also when the distance between the current state $x(t)$ and the actual equilibrium point x_i^{eq} significantly increases. To this end, let $\mathcal{T}_i\subset\mathbb{R}^n$ be the set of states such that the $i-th$ linearized model retains its validity in terms of nonlinear system trajectory approximation and let $\bar{t}$ the actual instant when using $CG_{(i,\ j)}$. Then, if $x(\bar{t})\notin\mathcal{T}_i$ a switching amongst the CG candidates takes place by means of the *Switching procedure*. The set $\mathcal{T}_i$ can be obtained by resorting to linearization arguments, see (10)-(11), in terms of semi-algebraic conditions. By noting that an equivalent description of this set of states can be given by deriving an appropriate normalized polynomial level surface function $V(z)$ in the extended space $z:=[\delta x_p^T,\ \delta u^T]^T$, i.e.

$$\mathcal{T}_i:=\text{Proj}_X\{z\in\mathbb{R}^{n+m},\,|\,V_i(z)\leq 1\}, \tag{27}$$

where Proj_X is the projection onto X. Then, by exploiting the requirements (11), there exists a polynomial level surface function $V_i(z)$ for the semi-algebraic set $\{z\in\mathbb{R}^{n+m}\,|\,V_i(z)\leq 1\}$ if the following set inclusion holds

$$\begin{aligned}&\{z\in\mathbb{R}^{n+m},\,|\,V_i(z)\leq 1\}\cap\{z\in\mathbb{R}^{n+m},\,|\,z^T z\leq r_z^{i^2}\}\\&\subseteq\{z\in\mathbb{R}^{n+m}\,|\,F_i(z)^T F_i(z)\leq\gamma_z^{i^2}\}\end{aligned} \tag{28}$$

The computation of $\mathcal{T}_i$ can be achieved by solving a Sum-of-Squares optimization problem, see [32]. □

IV. Real-time Hybrid Command Governor (RT-HCG) scheme

In this section a supervisory CG-based real-time scheme for the proposed architecture is detailed. Given a set of operating points $\{(x_i^{eq},u_i^{eq})\}_{i=1}^N$ for (9), we will assume that: To precisely state the overall control framework, the following assumptions are made:

B1 - At each time instant t, the supervisory unit is informed on the current plant structure;

B2 - The time interval T_{ON}, necessary for the on-line computation of the CG action is such that $T_{ON}<T_s$, with T_s the sampling time;

The idea we want to develop can be summarized as follows.

RT-HCG Strategy - *At the generic time instant t, the plant is under the action of the $CG_{(i,\ j)}$ unit and the supervisor receives the information on the plant structure to be fulfilled at $t+1$. The supervisor logic retains valid the $CG_{(i,\ j)}$ unit as long as the distance between the equilibrium x_i^{eq} and the actual state $x(t)$ is minimal and the constraint configuration is unchanged. The supervisor switches according to:*

- *Set-point Change - The selected unit is $CG_{(i',\ j)}$ unit where i' is chosen according to the rule*

$$i':=\underset{k}{\text{argmin}}\|x_k^{eq}-x(t)\| \tag{29}$$

- *Constraints Change - The selected unit is $CG_{(i,\ j')}$ if a constraint configuration $\mathcal{C}_{j'}\neq\mathcal{C}_j$ occurs.*

The supervisor scheme is depicted in Fig. 5: $r(t|t+1)$ is the reference known at the time instant t and to be tracked at $t+1$, $\mathcal{C}_{t,t+1}$ is the constraint configuration known at t and to be fulfilled at $t+1$ and $r(t)$, $x(t)$ are the reference and state measurements. The following distinct events may occur:

- *Set-point change (state transition* **new-eq**, Fig. 6) -
  If $r(t|t+1)\notin\mathcal{W}^{\delta}_{(i,\ j)}$, a switching to the $i'-th$ linearized model selected by (29) must be imposed. Then, the time interval $[t,\ t+1]$, is divided in two parts: the first is used to compute the new command $g(t)$ via the $CG_{(i,\ j)}$ device, while the lasting part is exploited for the computation of the new $CG_{(i',\ j)}$ unit.
  Note that even if $r(t|t+1)\notin\mathcal{W}^{\delta}_{(i,\ j)}$, this does not represent an hitch because in view of the properties (13) and (14), there always exists a sequence of CG units able to comply with the set-point requirement. Fig. 2 depicts the conditions under which the $CG_{(i,\ j)}\rightarrow CG_{(i',\ j)}$ switching is admissible;

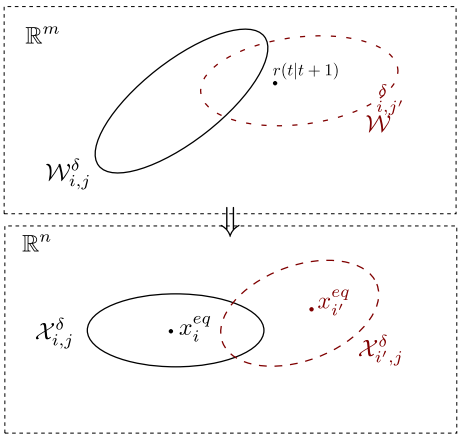

Fig. 2. Set-point change switching

- *Constraint configuration change (state transition* **new-conf**, Fig. 6) -
  Because the on-line design of the $CG_{(i',\ j)}$ unit could require more than one sampling time and the action of $CG_{(i,\ j)}$ is no longer admissible, to guarantee constraint fulfilment at each time instant t an adequate controller must be considered. Such a regulator, in place of the primal control law K_i and the $CG_{(i,\ j)}$ device, should

be capable to satisfy all the constraints regardless set-point tracking properties until the $CG_{(i',\ j)}$ computation phase is accomplished. Hereafter, we denote it as the *safe controller* K_{safe} (see Appendix B).
In Fig. 3 it is shown that if $\mathcal{C}_j \cap \mathcal{C}_{j'} \neq \emptyset$ then the same holds true for both $\mathcal{W}^{\delta}_{(i,\ j)} \cap \mathcal{W}^{\delta}_{(i,\ j')}$ and $\mathcal{X}^{\delta}_{(i,\ j)} \cap \mathcal{W}^{\delta}_{(i,\ j')}$. As a consequence the $CG_{(i,\ j)} \rightarrow CG_{(i,\ j')}$ switching can be carried out.

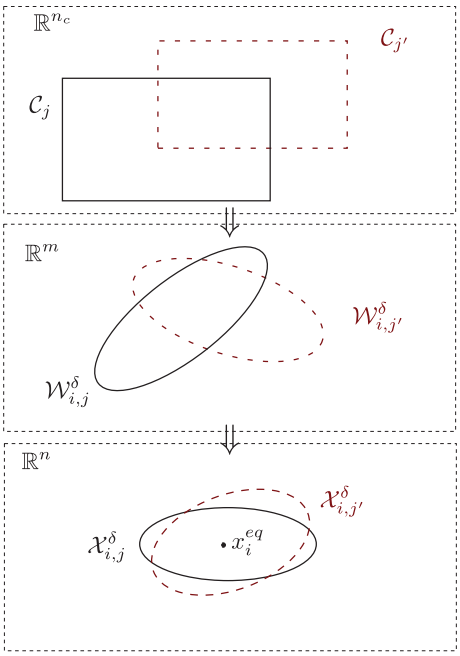

Fig. 3. Constraint configuration change switching

- *Equilibrium change (state transition* **new-eq**, Fig. 6) - By checking (18) it results that a switching to the $i'-th$ model is more adequate to approximate the plant behavior (9). Then, the time interval $[t,\ t+1]$, is split in two fractions: the first portion is used to compute $g(t)$ by using the current reference governor $CG_{(i,\ j)}$, while the remaining available computation time is used to begin with the derivation of the $CG_{(i',\ j)}$ unit. Finally, Fig. 4 describes the requirements under which it is possible to perform the $CG_{(i,\ j)} \rightarrow CG_{(i',\ j)}$ switching.

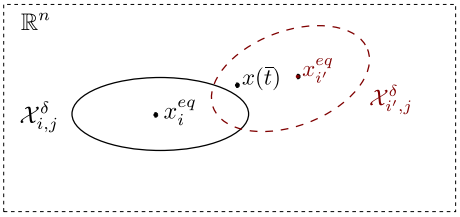

Fig. 4. Equilibrium change switching

A. Supervisor finite state automaton

The aim of this section is to outline the discrete event part of the proposed real-time CG architecture. To this end, the *Supervisor* behaviour can be described by means of a finite

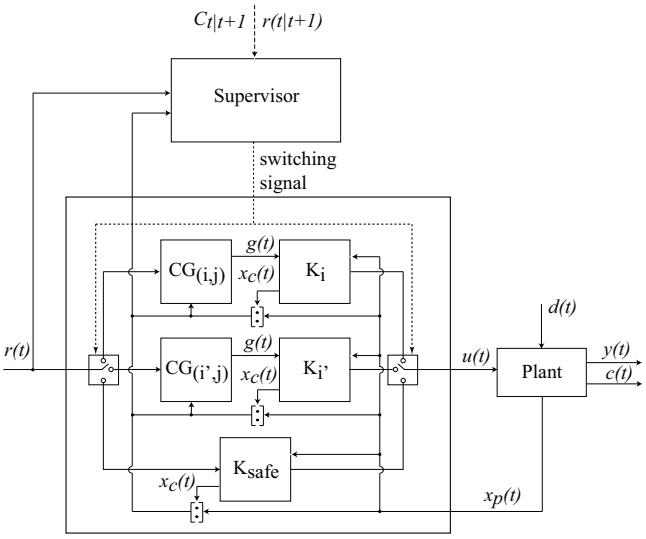

Fig. 5. Supervisory scheme

state automaton as detailed in Fig. 6. Specifically, three operating states are defined: **HOME**: normal operating condition under a CG unit action; **EQ-SW**: handling of a set-point or an equilibrium point change event; **CNF-SW**: handling of a constraint configuration change event.
The *Supervisor* is set by default to the **HOME** state where

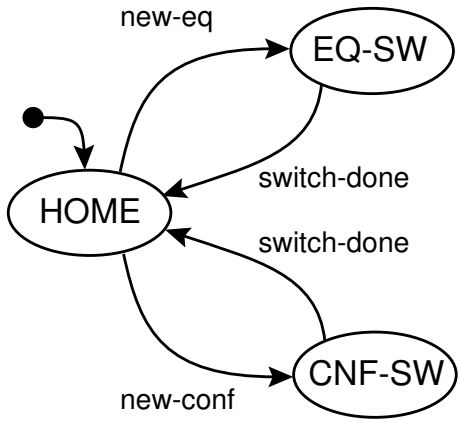

Fig. 6. *Supervisor* automaton

the control action is carried out by a single periodic task $\tau_{CG_{(i,\ j)}}$ (Fig. 7) which runs at the highest priority level and executes all the CG operations. In particular, the $\tau_{CG_{(i,\ j)}}$ actions are: reference and state measurements acquisition, on-line computation of the reference governor output $g(t)$, primal controller execution and application of $g(t)$.

Fig. 7. Task scheduling (HOME state)

If the set-point or an equilibrium point change occurrence is detected (**new-eq** event) the *Supervisor* switches to the **EQ-**

SW state where the operation mode enables the computation of the new CG design. In particular the transition **HOME** $\rightarrow$ **EQ-SW** occurs when one of the following two events take place: $x(t) \notin \mathcal{T}_i$ or $r(t|t+1) \neq r(t)$ and $r(t|t+1) \notin \mathcal{W}^{\delta}_{(i,\ j)}$. Then $i' = \underset{k}{\operatorname{argmin}} \|x^{eq}_k - x(t)\|$, $i' \neq i$, and the $CG_{(i',\ j)}$ is designed under the condition $Int\{\mathcal{W}^{\delta}_{(i,\ j)} \cap \mathcal{W}^{\delta}_{(i',\ j)}\} \neq \emptyset$.
From a real-time perspective, the design of the CG is assigned to an aperiodic task τ_{SW} which is released when **EQ-SW** becomes active and runs at a lower priority level with respect to $\tau_{CG_{(i,\ j)}}$. In the general case (see Fig. 8), τ_{SW} is not able to complete its task (CG design) within a single sampling period because a fraction of this time interval must be used for the execution of $\tau_{CG_{(i,\ j)}}$. Therefore, the process τ_{SW} is pre-empted a certain number of times by $\tau_{CG_{(i,\ j)}}$. As soon as the task τ_{SW} accomplishes its job (**switch-done** event), the *Supervisor* switches to the new $CG_{(i',\ j)}$, and the system operation mode is set to **HOME**.

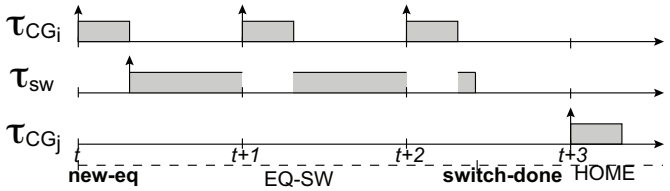

Fig. 8. Task scheduling (EQ-SW state)

A different mode transition occurs when a constraint configuration change is detected (**new-conf** event), i.e. **HOME** $\rightarrow$ **CNF-SW**, where the one-step ahead constraint configuration is such that $\mathcal{C}_{j'} =: \mathcal{C}_{t|t+1} \nsubseteq \mathcal{C}_j$, and, thanking to (20), we have that $\mathcal{C}_{t|t+1} \cap \mathcal{C}_j \neq \emptyset$.
In this case, the CG design is accomplished by an aperiodic task instance τ_{SW}. On the other hand, at the actual time instant t (see Fig. 9), the actions provided by $\tau_{CG_{(i,\ j)}}$ are not adequate because the fulfilment of the new constraint set is no longer guaranteed. Then, within $[t,\ t+1]$ the *Supervisor* establishes the execution of a new task , denoted as τ_{CS}, whose actions are: computation of K_{safe} and its application in order to ensure at least constraint satisfaction. At each future sampling time $[t+i,\ t+1+i],\ i \geq 1$, a periodic task τ_{safe} is in charge to manage the control action due to K_{safe}. Note that both τ_{CS} and τ_{safe} tasks inherit the priority level of $\tau_{CG_{(i,\ j)}}$. Finally, when the τ_{SW} (**switch-done** event) ends, the *Supervisor* de-schedules τ_{safe}. The task $\tau_{CG_{(i,\ j)}}$ is now restarted and equipped with the new on-line computed CG. The system operation mode is then reset to the **HOME** state.

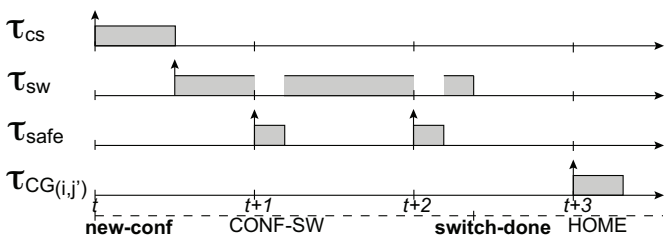

Fig. 9. Task scheduling (CNF-SW state)

B. Main results for RT-HCG

The main properties of the **RT-HCG** strategy are summarized in the next Proposition.

Proposition 3: Suppose that assumptions **A1**, **A2**, **B1**, **B2**, (13)-(14) for the time-varying set-point scenario and the Property 1 for the time-varying constraint scenario hold. Then:

- *No constraint configuration change occurrences* - All the properties of the CG device (see [2] Theorem 1, pg. 345) are preserved.
- *Constraint configuration change occurrences* - The K_{safe} controller guarantees "plant workability": asymptotic stability and constraint fulfilment.

Proof - Under no constraint configuration change, the overlapping condition (14) directly guarantees viability property by resorting to similar arguments as in [5]. During a constraint configuration change, its fulfilment and the stability are never lost due to the controller K_{safe}. On the contrary tracking performance may be lost because the system behaves essentially in an open-loop fashion. Finally, because this phase lasts for a finite time period tracking operations can be safely recovered by connecting the CG unit associated with the new constraint configuration. □

V. Experiments

Two numerical examples are used to validate the performance of the proposed supervisory strategy. First, a laboratory experiment which allows to evaluate the effectiveness of the **RT-HCG** scheme on a real process is presented. Then, simulations on a Cessna 182 aircraft model, used as a more complex example, are shown. The implementation and experimental results are discussed in the next subsections.

A. The four-tank process physical model

A laboratory four-tank process is used to evaluate the performance of the proposed **RT-HCG** supervisory strategy.

A mathematical representation for the four tank process is first derived by resorting to input/output measurements and geometrical/physical data. The goal is to regulate the water levels $h_3(t)$ and $h_4(t)$ (plant outputs) at given set-points by acting on the incoming water flows via the supply pump voltages $V_1(t)$ and $V_2(t)$ (plant inputs).

The geometrical parameters (length, height and width) of the four tanks (Fig. 10) are $12.15\,cm$, $23\,cm$, and $7.7\,cm$, respectively. The pumps are Rule$^{\text{TM}}$ 360 GPH type, having a 12 Volts supply voltage and the water tank levels are measured by using pressure transducers Cerabar$^{\text{TM}}$ T PMP 131 model. The tanks and the pumps are connected by flexible plastic pipes, whose diameters are $d_1 = d_2 = 2\,cm$, $d_{13} = d_{24} = d_3 = d_4 = 0.98\,cm$ and $d_{14} = d_{23} = 0.75\,cm$.

A nonlinear process model could be achieved by using mass balance and Bernoulli's law

$$\begin{cases} \frac{dh_1}{dt} = -\mu_1 \frac{a_{13}}{A_1}\sqrt{2\,g\,h_1} - \mu_1 \frac{a_{14}}{A_1}\sqrt{2\,g\,h_1} + \frac{1}{A_1}\,q_1(V_1) \\ \frac{dh_2}{dt} = -\mu_2 \frac{a_{23}}{A_2}\sqrt{2\,g\,h_2} - \mu_2 \frac{a_{24}}{A_2}\sqrt{2\,g\,h_2} + \frac{1}{A_2}\,q_2(V_2) \\ \frac{dh_3}{dt} = -\mu_3 \frac{a_3}{A_3}\sqrt{2\,g\,h_3} - \mu_{13} \frac{a_{13}}{A_3}\sqrt{2\,g\,h_1} + \mu_{23} \frac{a_{23}}{A_3}\sqrt{2\,g\,h_2} \\ \frac{dh_4}{dt} = -\mu_4 \frac{a4}{A_4}\sqrt{2\,g\,h_4} - \mu_{14} \frac{a_{14}}{A_4}\sqrt{2\,g\,h_1} + \mu_{24} \frac{a_{24}}{A_4}\sqrt{2\,g\,h_2} \end{cases} \quad (30)$$

Fig. 10. The laboratory four tanks process.

where $A_i = 93.555\,cm^2$, $i = 1,\ldots,4$, $a_3 = a_4 = a_{13} = a_{24} = 0.754\,cm^2$, $a_{14} = a_{23} = 0.442\,cm^2$ are the tanks and outlet hole cross-section areas and h_i, $i = 1,\ldots,4$ the water levels, respectively. The supply voltage to the i-th pump is V_i, the corresponding output water flow is given by the nonlinear law $q_i(V_i)$ and the gravity acceleration is denoted by g.

The μ_i coefficients are used for taking into consideration the effects of water turbulence, real pipe water flows and other model uncertainties. Such factors cannot be avoided in an accurate system modelling and their numerical values are not so simple to be determined. In order to overcome such a drawback, the idea here developed is to resort to a gray-box identification process by considering the following mathematical model for the four-tank process

$$\begin{cases} \frac{dh_1}{dt} &= -\alpha_1\sqrt{h_1} + \beta_1 V_1 + \beta_{1o} \\ \frac{dh_2}{dt} &= -\alpha_2\sqrt{h_2} + \beta_2 V_2 + \beta_{2o} \\ \frac{dh_3}{dt} &= \alpha_{13}\sqrt{h_1} + \alpha_{23}\sqrt{h_2} - \alpha_3\sqrt{h_3} \\ \frac{dh_3}{dt} &= \alpha_{14}\sqrt{h_1} + \alpha_{24}\sqrt{h_2} - \alpha_4\sqrt{h_4} \end{cases} \tag{31}$$

where

$$\alpha_1 = \tfrac{1}{A_1}\sqrt{2\,g}\,(\mu_1(a_{13}+a_{14}))\,, \alpha_2 = \tfrac{1}{A_2}\sqrt{2\,g}\,(\mu_1(a_{23}+a_{24}))$$
$$\alpha_{1_3} = \tfrac{1}{A_3}\sqrt{2\,g}\,(\mu_{13}a_{13})\,,\ \alpha_{2_3} = \tfrac{1}{A_3}\sqrt{2\,g}\,(\mu_{23}a_{23})$$
$$\alpha_3 = \tfrac{1}{A_3}\sqrt{2\,g}\,(\mu_3 a_3)\,,\ \alpha_{1_4} = \tfrac{1}{A_4}\sqrt{2\,g}\,(\mu_{14}a_{14})$$
$$\alpha_{2_4} = \tfrac{1}{A_4}\sqrt{2\,g}\,(\mu_{24}a_{24})\,,\ \alpha_4 = \tfrac{1}{A_4}\sqrt{2\,g}\,(\mu_4 a_4)\,,$$
$$\beta_i = \tfrac{k_i}{A_i}, i = 1,2.$$

Based on experimental tests, it has been determined that the pumps operate in linear regimes when restricted within the voltage range $[6,\ 8]\,Volt$. As a consequence, we will put those constraints on pump voltages and will consider the following linear relationship between the input voltages $V_i(t)$ and the incoming water flows $q_i(V_i(t))$, i.e. $q_i(t) = k_i\,V_i(t),\ i = 1,2$. Moreover, the parameters $\beta_{io} = \frac{k_{io}}{A_i}, i = 1,2$, along with the coefficients k_{io}, will be treated as offsets and added to take into account such a simplified linear behavior. The models (eq. (31)), obtained from the identification process fully described and analyzed in [11] are listed in Table I.

TABLE I
ESTIMATED PARAMETERS OF THE MODEL (31)

α_1	0.0713	β_1	0.1769	β_{1o}	-1.2102
α_2	0.1232	β_2	0.107	β_{2o}	-0.6021
α_3	0.2937	α_{13}	0.4870	α_{23}	0.2429
α_4	0.2348	α_{14}	0.2127	α_{24}	0.3146

The four-tank process has been fully described and analyzed in [11] under the assumption that the pumps operate in linear regimes within the range $[6,\ 8]\,Volt$. and the supervisory HCG strategy has been implemented on a real time computing unit. For HCG design purposes, the model (31) has been linearized around the following three equilibrium points:

$$x_1^{eq} = [0.6065\ 1.3050\ 5\ 5]^T, \quad u_1^{eq} = [7.1550\ 6.9424]^T,$$
$$x_2^{eq} = [1.0310\ 2.2185\ 8.5\ 8.5]^T, \quad u_2^{eq} = [7.2504\ 7.3421]^T,$$
$$x_3^{eq} = [1.6981\ 3.6540\ 14\ 14]^T, \quad u_3^{eq} = [7.3664\ 7.8281]^T,$$

where $x(t) = [h_1(t)\,h_2(t)\,h_3(t)\,h_4(t)]^T$ and $u(t) = [V_1(t)\ V_2(t)]^T$. Then, the linearized models have been discretized using forward Euler differences with a sampling time $T_s = 0.1\,s$ and physical constraints on maximum water levels and maximum pump supply voltage have been considered: $h_i(t) \le 16,\,[cm],\ i = 1,\ldots,4$ and $6 \le V_i(t) \le 8,\,[Volt],\ i = 1,2$. The following CG parameters, $\delta_i = 10^{-6}$, $i = 1,2,3$, and $\Psi = I_2$ have been chosen and the constraint horizon $k_0 = 130$ was computed via the numerical procedure proposed in [16]. Further, in order to characterize the set of admissible disturbances/measurement errors acting on the four tanks, the following convex and compact region has been considered and used in the CG setting:

$$\mathcal{D} := \left\{d \in \mathbb{R}^4 \mid Ud \le h\right\},$$

where $U = \begin{bmatrix} I_4 \\ -I_4 \end{bmatrix}$, $h = 0.3 * [1\ 1\ 1\ 1\ 1\ 1\ 1\ 1]^T\ \ [cm]$. The primal compensators $K_i, i = 1,2,3$, have been designed as two-degree of freedom LQ controllers. For comparison purposes a single CG unit has been off-line designed by referring to the equilibrium $(x_1^{eq},\ u_1^{eq})$. The following scenario has been taken into consideration:

Starting from $x(0) = [0.5458\ 1.1745\ 4.5\ \ 4.5]^T$, *the set-points* $h_{3ref} = h_{4ref} = 14.5\,cm$ *are first considered. Then at* $210\,s$ *a set-point change (*$h_{3ref} = h_{4ref} = 10\,cm$*) and a constraint configuration change (*$0.5 \le h_i(t) \le 15,\,[cm],\ i = 1,2$ *and* $9.5 \le h_i(t) \le 15,\,[cm],\ i = 3,4$*) jointly occur.*

All the experiments are reported in Figs. 11-13. As it results the HGC device is capable to adequately comply both with the tracking requirements of the first phase $[0,\ 210]\,s$ and the successive time-varying scenario. It can be observed in fact that (Fig. 11) first both the Tanks 3 and 4 settle down to the prescribed set-points and then such a strategy is capable to deal with the new set-point/constraint configuration without constraint violation, see also Fig. 12. This is clearly achieved by means of appropriate CG switchings as highlighted in Fig.

TABLE II
COMPUTATIONAL LOADS (MS)

State	Min.	Max.
HOME	0.8	1.6
EQ-SW	24.8	39.2
CNF-SW	24.8	39.2

13. In particular, it is interesting to note that at $t = 40\,sec.$ the switching $CG_{(2,1)} \rightarrow CG_{(3,1)}$ occurs in view of **Remark 1** arguments: because $\mathcal{T}_2 = \{\delta_x : \delta_x^T \delta_x \leq 0.15\}$, $\mathcal{T}_3 = \{\delta_x : \delta_x^T \delta_x \leq 0.1\}$ and the state measurement $x(40) = [2.52,\ 3.23,\ 14.05,\ 12.32]^T$, we have that $x(40) - x_2^{eq} \notin \mathcal{T}_2$ and $x(40) - x_3^{eq} \in \mathcal{T}_3$.
Conversely, the single $CG_{(1,1)}$ action is not capable to settle down to $14.5\,cm$ because $h_{iref} = 14.5\,cm$, $i = 3, 4$, do not belong to $\mathcal{W}_1^{\delta}$. Moreover, as expected, the time varying scenario cannot be managed by $CG_{(1,1)}$ and therefore constraint violations occur (Fig. 11).
Finally, a computational load analysis has been carried out. Note that: 1) algebraic computations have been performed by means of uBLAS [7]; 2) the CG output $g(t)$ has been achieved by solving a QP optimization problem via a C++ implementation of the algorithm proposed in [20]; 3) the real-time framework is the RTAI v. 3.5 hosted on a i386 Linux Kernel v. 2.6.19 architecture running on a Sony Vaio (Intel i5 - $2.5\,GHz$, $2\,GB$ ram). Table II reports the minimum/maximum computation times needed to execute the tasks associated to each automaton state at each time instant t.

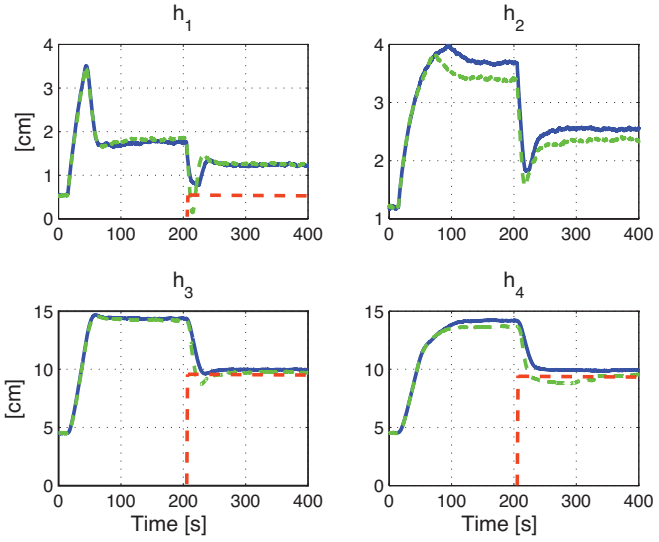

Fig. 11. Water levels behaviours: solid-line with HCG and dot-line with $CG_{(1,1)}$. Prescribed constraints: dashed lines.

B. Aircraft flight control

In this section the HCG strategy is applied to the speed and attitude control of a light utility aircraft, namely the Cessna 182 subject to angle of attack and surface deflection constraints. By using the lines indicated in [30], the 3-DOF longitudinal model of the aircraft motion dynamics is

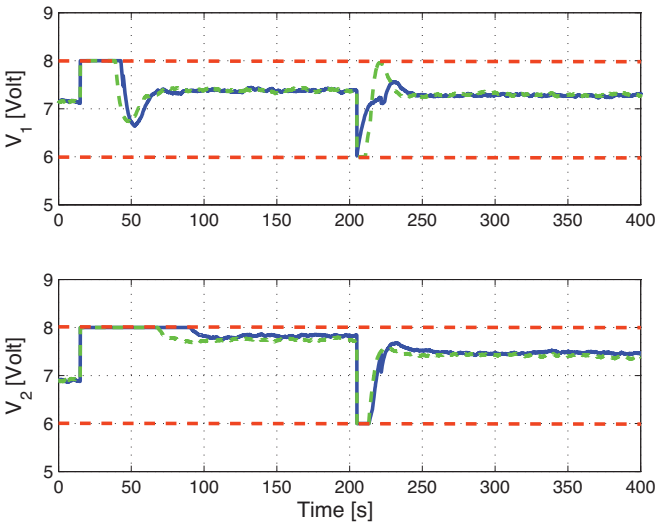

Fig. 12. Voltages provided by the pumps: solid-line with HCG and dot-line with $CG_{(1,1)}$. Prescribed constraints: dashed lines.

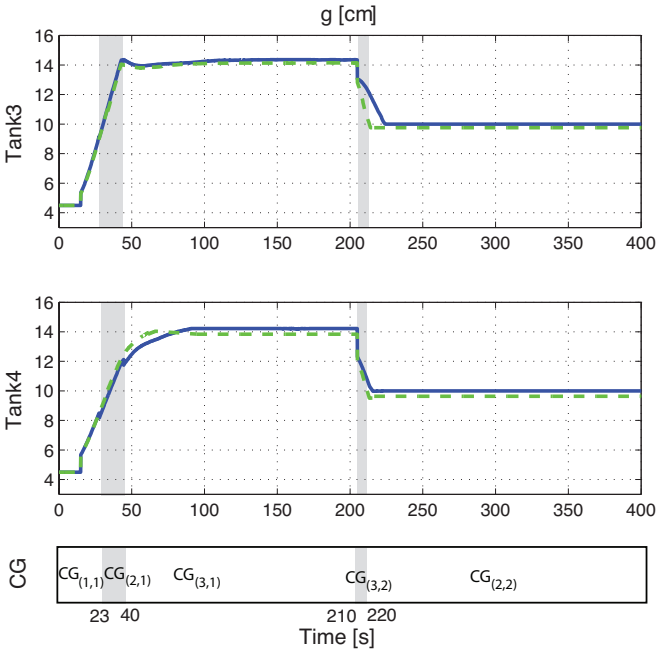

Fig. 13. Outputs of HCG and $CG_{(1,1)}$ units

described by the following equations

$$\dot{v} = -\frac{\rho v^2 S_w}{2m}(C_{D_0} + C_{D_\alpha}\alpha + C_{D_q}\frac{q\bar{c}}{2v} + C_{D_{\delta_e}}\delta_e) + \frac{T}{m}\cos\alpha - g\sin(\theta - \alpha) \quad (32)$$

$$\dot{\alpha} = q - \frac{\rho v^2 S_w}{2mv}(C_{L_0} + C_{L_\alpha}\alpha + C_{L_q}\frac{q\bar{c}}{2v} + C_{L_{\delta_e}}\delta_e) - \frac{T}{mv}\sin\alpha + \frac{g}{v}\cos(\theta - \alpha) \quad (33)$$

$$\dot{q} = \frac{\rho v^2 S_w \bar{c}}{2I_{yy}}(C_{m_0} + C_{m_\alpha}\alpha + C_{m_q}\frac{q\bar{c}}{2v} + C_{m_{\delta_e}}\delta_e) \quad (34)$$

$$\dot{\theta} = q \quad (35)$$

$$\dot{h} = -v\sin(\theta - \alpha) \quad (36)$$

Note that such a description belongs to the class of plant models (9) with $x_p(t) = [v(t)\ \alpha(t)\ q(t)\ \theta(t)]^T$ and $u(t) = [T(t)\ \delta_e(t)]^T$. Meaning of the involved variables and parameters are standard and are reported in [30]. Moreover, as primal controllers we have designed optimal control laws including integrals to regulate velocity and pitch angle state variables.

In the proposed numerical simulation, we have considered:

- ten equilibrium points:

$$x_1^{eq} = [32.9\,0.24\,0\,0.24]^T, \quad x_2^{eq} = [34.7\,0.208\,0\,0.21]^T$$
$$u_1^{eq} = [508\ \ -0.096]^T, \quad u_2^{eq} = [600\ \ -0.08]^T$$

$$x_3^{eq} = [40\,0.14\,0\,0.14]^T, \quad x_4^{eq} = [43.6\,0.104\,0\,0.103]^T$$
$$u_3^{eq} = [575\ \ -0.04]^T, \quad u_4^{eq} = [600\ \ -0.021]^T$$

$$x_5^{eq} = [37.8\,0.164\,0\,0.164]^T, \quad x_6^{eq} = [45\,0.093\,0\,0.091]^T$$
$$u_5^{eq} = [551\ \ -0.05]^T, \quad u_6^{eq} = [600\ \ -0.015]^T$$

$$x_7^{eq} = [47.6\,0.075\,0\,0.075]^T, \quad x_8^{eq} = [50.1\,0.06\,0\,0.06]^T$$
$$u_7^{eq} = [667\ \ -0.006]^T, \quad u_8^{eq} = [701\,0.002]^T$$

$$x_9^{eq} = [52.5\,0.048\,0\,0.048]^T, \quad x_{10}^{eq} = [55\,0.037\,0\,0.037]^T$$
$$u_9^{eq} = [738\,0.009]^T, \quad u_{10}^{eq} = [776\,0.015]^T$$

- a sampling time $T_s = 0.001\,s$;
- physical constraints below reported:

$$18.13 \leq \ v \ \leq 77\ [m/sec] \tag{37}$$
$$-0.26 \leq \ \alpha \ \leq 0.26\ [rad] \tag{38}$$
$$-1.75 \leq \ q \ \leq 1.75\ [rad/sec] \tag{39}$$
$$-0.7 \leq \ \theta \ \leq 0.7\ [rad] \tag{40}$$
$$0 \leq \ T \ \leq 2357.2\ [N] \tag{41}$$
$$-0.48 \leq \ \delta_e \ \leq 0.48\ [rad] \tag{42}$$

Then, the following flight scenario has been used for simulation purposes:
The reference velocity and the reference pitch attitude angle are initially set to $v_{ref} = 38.95\,m/s$ and $\theta_{ref} = 0.15\,rad$ respectively. Then, both references are linearly interpolated between $t = 7\,s$ and $t = 12.5\,s$ to reach the final set-points $v_{ref} = 55\,m/s$ and $\theta_{ref} = 0.037\,rad$. The initial state condition is chosen as $x(0) = [36.9\ 0.177\ 0.00\ 0.177]^T$.
The chosen knobs of the CG units are $\delta_i = 10^{-6}$, $i = 1, \ldots, 4$, and $\Psi = I_2$, while the constraint horizon is equal to $k_0 = 200$. The numerical results are reported in Figs. 14-15, where comparisons with the dynamical behaviours obtained without the action of the **RT-HCG** are presented. Recall that physical saturations of the aircraft input are taken into account: see constraints (41) and (42). Moreover it is interesting to underline that the two schemes identically behave until the first CG switching occurrence, i.e. at $t = 10.3521\,s$ $CG_{(1,1)} \rightarrow CG_{(2,1)}$. The observed behaviour is compliant with the CG philosophy because if constraints violations do not occur the CG becomes *transparent* with respect to the primal controller action, see Figs. 14-15.

Comparisons put in light two main phenomena deserving specific attention. Around $t = 11\,s$, an attempt to track the velocity reference is observed, the prescribed upper limit on the thrust is quite quickly reached when the **RT-HCG** unit is disconnected and thereby the saturations give rise to the oscillations shown in Fig. 14 (angle of attack: the upper-right subplot). This irregular behaviour is avoided when a proper **RT-HCG** unit is added: thanking to the capability of the proposed **RT-HCG** strategy to apply control actions deriving by more accurate plant linearizations (CG swtichings) the drawbacks due to significant and sudden velocity variations can be mitigated. The second interesting situation is related to the inability of the aircraft to track the reference on the pitch attitude angle (lower-right subplot of Fig. 14) without the **RT-HCG** action and and, as a consequence, the Cessna 182 loses altitude as shown in Fig. 16. This critical event can be understood by recalling that the primal controller is designed with respect to the operating point (x_1^{eq}, u_1^{eq}) and the corresponding plant linearizion does not approximate the nonlinear Cessna 182 behaviour when the aircraft *sufficiently* departs from (x_1^{eq}, u_1^{eq}). This phenomenon does not occur under the **RT-HCG** action because it is capable to use a new CG unit which is on-line designed with respect to a compatible plant linearization. For the sake of completeness, we have then reported in Table III all the switching sequences during the on-line operations amongst the CG units that are computed by means of the Section 4 prescriptions.

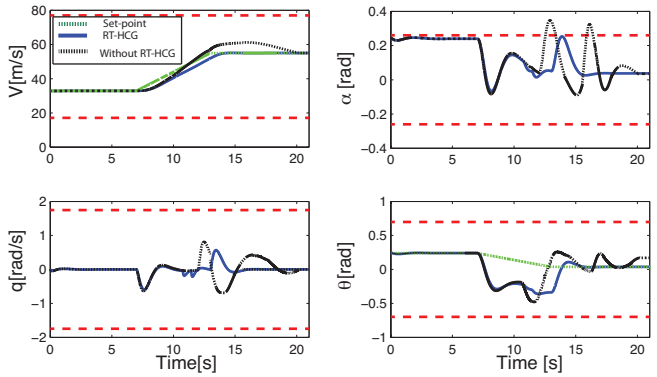

Fig. 14. Velocity, angle of attack, pitch attitude rate and pitch attitude angle. The dashed lines are the reference signals. The dash-dotted lines represent the prescribed constraints.

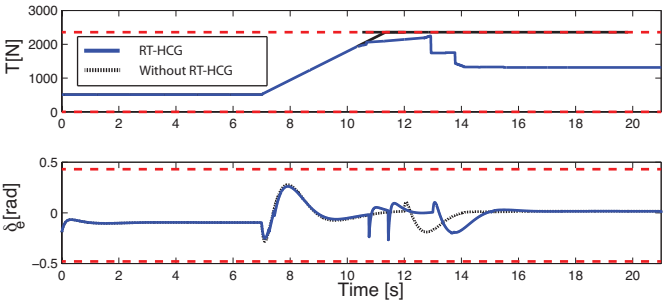

Fig. 15. Thrust and deflection angle. The dash-dotted lines represent the prescribed constraint.

Finally the minimum/maximum computation times are summarized in Table IV, where it results that the equilibrium change switching needs at least two sampling time intervals to be on-line completed. On the other hand, it must be underlined that the used sampling time ($T_s = 0.001\,s$) is smaller with

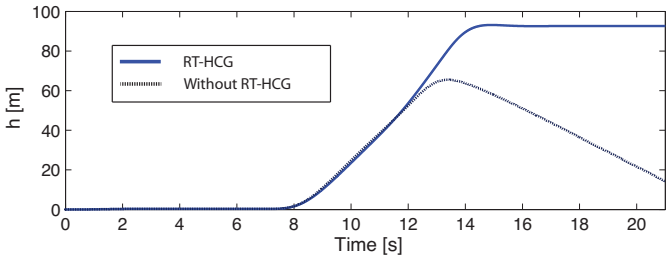

Fig. 16. Aircraft trajectory

TABLE III
CG SWITCHINGS

t	CG Transition
10.35	$CG_{(1,1)} \rightarrow CG_{(2,1)}$
14.11	$CG_{(2,1)} \rightarrow CG_{(3,1)}$
15.09	$CG_{(3,1)} \rightarrow CG_{(4,1)}$
18.22	$CG_{(4,1)} \rightarrow CG_{(8,1)}$
19.93	$CG_{(8,1)} \rightarrow CG_{(10,1)}$

TABLE IV
COMPUTATIONAL LOADS (MS)

State	Min.	Max.
HOME	0.3	0.6
EQ-SW	1.85	3.5

respect to non-critical choices (around $T_s = 0.01\ s$) with the consequence that the **RT-HCG** supervisory scheme is clearly able to improve the overall control performance.

VI. CONCLUSIONS

A real-time hybrid strategy for orchestrating switchings between CG units has been presented. The main feature is the ability to take care of both time-varying set-points and constraint scenarios by on-line computing the proper control architecture. This is achieved by resorting to a supervisory based framework that, on the basis of the available plant structure information, takes adequate decisions to ensure constraints satisfaction and to guarantee tracking properties. The applicability and effectiveness of the proposed supervisory scheme have been demonstrated by means of two applications that have put in evidence that the **RT-HCG** scheme is capable to on-line manage sudden changes in the operating conditions due to target and/or unexpected anomalies in the plant behaviour.

REFERENCES

[1] D. Angeli and E. Mosca, "Command governor for nonlinear systems under constraint", *IEEE Trans. Auto. Control*, Vol. 44, pp. 816-820, 1999.
[2] F. Bacconi, E. Mosca and A. Casavola, "Hybrid constrained formation flying control of micro-satellites", *IET Control Theory Appl.*, Vol. 1, No. 2, pp. 513-521, 2007.
[3] A. Bemporad, "Reference Governor fo Constrained Nonlinear Systems", *IEEE Trans. Auto. Control*, Vol. 43, pp. 415-419, 1998.
[4] A. Bemporad and E. Mosca, "Fulfilling Hard constraint in Uncertain Linear Systems by Reference Managing", *Automatica*, Vol. 34, pp. 451-461, 1998.
[5] A. Bemporad, A. Casavola and E. Mosca, "Nonlinear Control of Constrained Linear Systems via Predictive Reference Management," *IEEE Trans. Auto. Control*, Vol. 42, pp. 340-349, 1997.
[6] P. Tøndela, T. A. Johansen and A.Bemporad," An algorithm for multi-parametric quadratic programming and explicit MPC solutions ", *Automatica*, Vol. 39, No. 3, pp. 451-461, 2003.
[7] L. S. Blackford, J. Demmel, J. Dongarra, I. Duff, S. Hammarling, G. Henry, M. Heroux, L. Kaufman, A. Lumsdaine, A. Petitet, R. Pozo, K. Remington and R. C. Whaley, "An Updated Set of Basic Linear Algebra Subprograms (BLAS)", *ACM Trans. Math. Soft.*, 28-2, pp. 135-151, 2003.
[8] F. Blanchini and S. Miani. "Set-Theoretic Methods in Control", *Birkäuser*, Boston, 2008.
[9] S. Boyd, L. El Ghaoui, E. Feron and V. Balakrishnan, "Linear Matrix Inequalities in System and Control Theory", *SIAM Studies in Applied Mathematics*, 15, SIAM, London.
[10] M. S. Branicky,"Multiple Lyapunov Functions and Other Analysis Tools for Switched and Hybrid Systems", *IEEE Trans. Auto. Control*, Vol. 43, No. 4, pp. 475-482, 1998.
[11] A. Casavola, D. Famularo, G. Franzè and A. Furfaro. "A fault-tolerant real-time supervisory scheme for an interconneted four tanks process", 2010 ACC, Baltimore, Maryland, 2010.
[12] A. Dalvi and M. Guay, "Control and real-time optimization of anauto-motive hybrid fuel cell power system", *Contr. Eng. Practice*, Vol. 17, pp. 924-938, 2009.
[13] L. Dozio and P. Mantegazza, "Real Time Distributed Control Systems using RTAI", *Proceedings of the 6th IEEE International Symposium on Object-Oriented Real-Time Distributed Computing*, pp. 11-18, 2003, Hakodate, Hokkaido, Japan.
[14] M. Diehl, H. G. Bock, J. P. Schlder, R. Findeisen, Z. Nagy and F. Allgöwer, "Real-time optimization and nonlinear model predictive control of processes governed by differential-algebraic equations", *Journal of Process Control*, pp. 577–585, Vol. 14, 2002.
[15] A. Gambier, "Real-time control systems: A Tutorial", *Proceedings of the 5th Asian Control Conference*, 2004, Mebourne, Australia.
[16] E.G. Gilbert, I. Kolmanovsky and K. Tin Tan, "Discrete-time Reference Governors and the Nonlinear Control of Systems with State and Control constraint", *International Journal on Robust and Nonlinear Control*, Vol. 5, pp. 487-504, 1995.
[17] E.G. Gilbert and I. Kolmanovsky, "Fast reference governors for systems with state and control constraint and disturbance inputs", *Int. J. on Rob. and Nonlinear Contr.*, Vol. 9, pp. 1117-1141, 1999.
[18] H.K. Khalil, "Nonlinear Systems", *Prentice Hall*, 1996.
[19] E.G. Gilbert and K. Tin Tan, "Linear systems with state and control constraint: the theory and applications of maximal output admissible sets", *IEEE Tran.s Aut. Contr.*, Vol. 36, pp. 1008-1020, 1991.
[20] D. Goldfarb and A. Idnani, "A numerically stable dual method for solving strictly convex quadratic programs", *Math. Program.*, vol. 27, pp. 133, 1983.
[21] G. C. Goodwin, "Defining the performance envelope in industrial control", 16-th American Control Conference, Albuquerque, NM, 1997, Plenary Session 1.
[22] C. Guo and Q. Song, "Real-Time Control of Variable Air Volume System Based on a Robust Neural Network Assisted PI Controller", *IEEE Trans. Cont. Sys. Tech.*, vol. 17, pp. 600-607, 2009.
[23] A. Kurzhanski and I. Valyi. "Ellipsoidal calculus for estimation and control", *Birkäuser*, Boston, 1996.
[24] R. Mall, "Real-Time Systems: Theory and Practice", Pearson Ed., 2006.
[25] M. Mattei, C. V. Labate and D. Famularo, "A constrained control strategy for the shape control in thermonuclear fusion tokamaks", *Automatica*, Vol. 19, No. 1, pp. 169-177, 2013.
[26] T. Micksh, A. Gambier and E. Badreddin, "Real-time Implementation of Fault-tolerant Control Using Model Predictive Control", in *Proceedings of the17th IFAC World Congress*, Seoul, Korea, pp. 11136-11141, 2008.
[27] R.H. Miller, I. Kolmanovsky, E.G. Gilbert and P.D. Washabaugh, "Control of constrained nonlinear systems: a case study", *IEEE Control Systems Magazine*, Vol. 20, pp. 23-32, 2000.
[28] S. J. Qin and T. A. Badgwell, "A survey of industrial model predictive control technology", *Control Engineering Practice*, Vol. 11, pp. 733–764, 2003.
[29] S.J. Park and J.M. Yang, "Supervisory control for real-time scheduling of periodic and sporadic tasks with resource constraint", *Automatica*, Vol. 45, No. 11, pp:2597–2604, 2009.
[30] A. Roskam, "Airplane Flight Dynamics and Automatic Flight Control Part I", 1985.
[31] RTAI. RealTime Application Interface for Linux. https://www.rtai.org/.
[32] W. Tan and A. Packard, "Stability region Analysis using polynomial and composite polynomial Lyapunov functions and Sum-of-Squares programming, *IEEE Trans. Auto. Contr.*, Vol. 53, pp. 565–571, 2008.
[33] Y. Wang and S. Boyd, "Fast Model Predictive Control Using Online Optimization" *IEEE Trans. Cont. Syst. Techn.*, Vol. 18, No. 2, pp. 267–278, 2010.
[34] P. Wen, J. Cao and Y. Li, "Design of high-performance networked real-time control systems" *IET, Control Theory & Applications*, Vol. 1, No. 5, pp. 1329–1335, 2007.

A Proof of Proposition 1

Because $\bar{x}_{\bar{w}}$ is an equilibrium point we have that

$$x_{\bar{w}} = (I - \Phi)^{-1} G\, \bar{w} + \tilde{x} \tag{43}$$

where $\tilde{x}$ is an additive perturbation such that $\|\tilde{x}\| \leq \xi$ with ξ sufficiently small. Let us suppose that once $x_{\bar{w}}$ has been reached, a new constraint scenario $\mathcal{C}^{\delta}_{j'}$, such that $\mathcal{C}^{\delta}_{j} \cap \mathcal{C}^{\delta}_{j'} \neq \emptyset$, occurs. In view of Property 1 (eq. (20)), a new command $\underline{w}$ such that $\underline{w} \in \mathcal{C}^{\delta}_{j} \cap \mathcal{C}^{\delta}_{j'}$ can be considered and the constrained vector becomes

$$c(k, x_{\bar{w}}, \underline{w}) = H_c \Phi^k \bar{x}_{\bar{w}} + H_c \sum_{l=0}^{k-1} \Phi^l G \underline{w} + L \underline{w} \tag{44}$$

Then by taking into account (43) we have

$$\begin{array}{l} c(k, x_{\bar{w}}, \underline{w}) = H_c \Phi^k \left(I - \Phi\right)^{-1} G\, \bar{w} + H_c \Phi^k \tilde{x} + \\ H_c \left(I - \Phi\right)^{-1} G \underline{w} + L \underline{w} - H_c \Phi^k \left(I - \Phi\right)^{-1} G \underline{w} \end{array}$$

from which

$$c(k, x_{\bar{w}}, \underline{w}) = c_{\underline{w}} + H_c \Phi^k \tilde{x} + H_c \left(I - \Phi\right)^{-1} G(\bar{w} - \underline{w}) \tag{45}$$

Because $\underline{w} \in \mathcal{C}^{\delta}_{i} \cap \mathcal{C}^{\delta}_{j}$, the constraint vector $c_{\bar{w}}$ fulfils the constraint scenario $\mathcal{C}^{\delta}_{j'}$ if

$$H_c \Phi^k \tilde{x} + H_c \left(I - \Phi\right)^{-1} G(\bar{w} - \underline{w}) \subset \mathcal{B}_{\delta}$$

that can be ensured by requiring that

$$\|\tilde{x}\| \leq \frac{\delta}{2\sigma(H_c)M} \text{ and } \|\bar{w} - \underline{w}\| \leq \frac{\delta(1-\lambda)}{2\sigma(H_c)\sigma(G)M^2}$$

where $\lambda \in [0, 1)$ is such that $\forall x \in \mathbb{R}^n$ one has that $\Phi^k x\| \leq M\lambda^k \|x\|,\ \forall k \in \mathbb{Z}_+$; $\sigma(H_c)$ and $\sigma(G)$ the maximum singular values of the matrices H_C and G respectively.

The conclusion is that starting sufficiently close to an equilibrium point $x_{\bar{w}},\ \bar{w} \in \mathcal{W}^{\delta}_{\bullet,j}$, if a switching to the constraint scenario $\mathcal{C}^{\delta}_{j'}$ occurs, in a finite time one can arrive as close as desired to any state $x_{\underline{w}} \in \mathcal{W}^{\delta}_{\bullet,j'}$ without constraint violation.

B The safe controller design

At the current instant $\hat{t}$, let $\mathcal{C}_j$ and $\mathcal{C}_{\hat{t}|\hat{t}+1}$ be the constraint and the one-step ahead constraint configurations, respectively. A safe controller K_{safe}, capable to ensure the constraint satisfaction from $\hat{t}+1$ onwards must be designed such that the switching from K_i to K_{safe} preserves asymptotic stability properties of the closed-loop system. The latter can be accomplished as follows. Let $\Xi_i := \{x \in \mathbb{R}^n \,|\, x^T P_i\, x \leq 1\}$ be the invariant region associated to the control law K_i and achieved by means of standard Lyapunov arguments. Then, because the switching from K_i to K_{safe} must also guarantee the asymptotic stability of the closed-loop system and the constraint satisfaction $c_i(t) \in \mathcal{C}_{\hat{t}|\hat{t}+1}, \forall t \geq \hat{t}+1$, the controller K_{safe} is computed by solving the following problem:

K_{safe} **Problem -** *Find a state feedback law K_{safe} and a positive definite matrix P_{safe} such that the following conditions hold true*

$$K_{safe} z \in U, \forall z \in \Xi_{safe} := \{x \in \mathbb{R}^n | x^T P_{safe} x \leq 1\} \subset X \tag{46}$$

$$x(\hat{t}) \in \Xi_i \cap \Xi_{safe} \tag{47}$$

where Ξ_{safe} is the ellipsoidal invariant set for the $i-th$ linearized system under the K_{safe} action. □

Note that the condition (47) is imposed to ensure the admissibility of the K_i-to-K_{safe} switching and it can be shown by exploiting the same arguments as e.g. in [10], while the requirement $\mathcal{C}_{\hat{t}|\hat{t}+1} \cap \mathcal{C}_j \neq \emptyset$ guarantees that $\Xi_i \cap \Xi_{safe} \neq \emptyset$. Finally, the numerical computation of K_{safe} can be obtained by solving an LMI feasibility problem, see [9] and [23]. □

Domenico Famularo Domenico Famularo received the Laurea degree in computer engineering from the University of Calabria, Italy, in 1991 and the Ph.D in computational mechanics from the University of Rome, Italy, in 1996. From 1991 to 2000 he was a Research Associate at the University of Calabria. In 1997 he was a visiting Scholar Research at the University of New Mexico (Albuquerque, NM, USA) and in 1999 he covered the same position at the University of Southern California (Los Angeles, CA). He was a Researcher at ICAR-CNR. and since 2005 he is an Associate Professor at the University of Calabria. His current research interests include control under constraints, control reconfiguration for fault tolerant systems and networked control systems.

Giuseppe Franze' Giuseppe Franzè was born in 1968 in Italy. He received the Ph.D. degree in systems engineering from the University of Calabria, Italy, in 1999. From 1994 to 2002 he was with the DEIS-University of Calabria, Italy, as an Assistant Researcher and since 2002 as an Assistant Professor. His current research interests include constrained predictive control, nonlinear systems, networked control systems, control under constraints and control reconfiguration for fault tolerant systems.

Angelo Furfaro Angelo Furfaro was born in 1974 in Italy. He received the Ph.D. degree in systems and computer engineering from the University of Calabria, Italy, in 2004. He is an Assistant Professor at the University of Calabria where he teaches Software Engineering and Embedded Devices Programming. His current research interests include modelling and simulation, model-checking and real-time systems.

Massimiliano Mattei Massimiliano Mattei received the Laurea degree in aeronautical engineering and the Ph.D. in electronic engineering from the University of Napoli Federico II in 1993 and 1997 respectively. Professor Mattei is an expert in the area of modeling and control of plasmas in thermonuclear fusion reactors. He regularly collaborates with JET, ITER, Fusion for Energy, EFDA, ENEA, and many other worldwide institutions in this area. His research interests also include flight control and autonomous vehicles guidance, control and navigation. He is a Professor of Flight Mechanics and Control at the Second University of Napoli where he is also the head of the Department of Industrial and Information Engineering.